Effective impedance modeling of metamaterial structures

Kokou B. Dossou*, Christopher G. Poulton and Lindsay C. Botten
Centre for Ultrahigh-Bandwidth Devices for Optical Systems (CUDOS), and School of Mathematical and Physical Sciences
University of Technology Sydney
PO Box 123, Broadway, New South Wales 2007, Australia
*Corresponding author: Kokou.Dossou@uts.edu.au

***Abstract*—We present methods for retrieving the effective impedance of metamaterials from the Fresnel reflection coefficients at the interface between two semi-infinite media. The derivation involves the projection of modal expansions onto the dominant modes of the two semi-infinite media. It is shown that a number of effective impedance formulas, previously obtained by field averaging techniques, can also be derived from the scattering-based formalism, by an appropriate choice of projection.**

I. Introduction

Effective medium techniques, when applicable, can provide deep physical insight into the properties of metamaterials and lead to simplified analytical treatments of these heterogeneous structures. The effective impedance of a medium can be retrieved from the Fresnel reflection coefficient [1], [2]. For the determination of the Fresnel reflection and transmission coefficients at the interface (see Fig. 1) between two semi-infinite media (1) and (2), the fields in each medium are represented by Bloch mode expansions. An orthogonality property can be used to transform the field matching conditions into a system of linear equations. When the wave propagation in each medium is dominated by a single mode, the projection of the rigorous modal expansions onto the set of dominant modes leads to a truncated system of two linear equations with two unknowns, which can be solved analytically to obtain the approximate reflection and transmission coefficients.

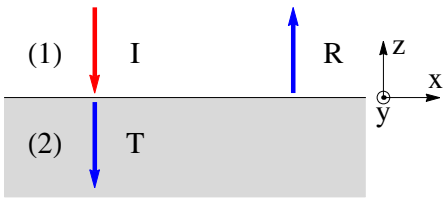

Fig. 1. Illustration of an incidence from a semi-infinite medium (1) into a semi-infinite medium (2).

II. The effective impedance

There exist a number of different effective impedance formulas and this reflects the fact that there are many variations in the implementation of the mode-matching techniques. If R and T are respectively the reflection and transmission coefficients, the tangential field continuity at the interface between the semi-infinite media can be written as

$$\boldsymbol{E}_\perp^{(1)-} + R\,\boldsymbol{E}_\perp^{(1)+} \approx T\,\boldsymbol{E}_\perp^{(2)-}, \quad (1)$$

$$\boldsymbol{H}_\perp^{(1)-} + R\,\boldsymbol{H}_\perp^{(1)+} \approx T\,\boldsymbol{H}_\perp^{(2)-}, \quad (2)$$

where $(\boldsymbol{E}^{(1)}, \boldsymbol{H}^{(1)})$ and $(\boldsymbol{E}^{(2)}, \boldsymbol{H}^{(2)})$ denotes respectively the dominant Bloch modes of the media (1) and (2). The mode-matching equations are obtained by projecting the modal expansions Eqs. (1) and (2) onto a set of test functions $\boldsymbol{E}_{\text{Test}}$ and $\boldsymbol{H}_{\text{Test}}$ (e.g., adjoint modes $\boldsymbol{E}^\dagger$ and $\boldsymbol{H}^\dagger$ [1]) and by applying the relevant the orthogonality properties. Several choices of test functions have been proposed and validated. For instance, the set of test functions can consist of:

1) The electric field of the adjoint mode from medium (1) and the magnetic field of the adjoint mode from medium (2): $\boldsymbol{E}_{\text{Test}} = \boldsymbol{E}^{(1)\dagger}$ and $\boldsymbol{H}_{\text{Test}} = \boldsymbol{H}^{(2)\dagger}$.
2) The electric field of the adjoint mode from medium (2) and the magnetic field of the adjoint mode from medium (1): $\boldsymbol{E}_{\text{Test}} = \boldsymbol{E}^{(2)\dagger}$ and $\boldsymbol{H}_{\text{Test}} = \boldsymbol{H}^{(1)\dagger}$.
3) Both the electric fields and magnetic fields of the adjoint mode from only medium (1): $\boldsymbol{E}_{\text{Test}} = \boldsymbol{E}^{(1)\dagger}$ and $\boldsymbol{H}_{\text{Test}} = \boldsymbol{H}^{(1)\dagger}$.

For normal incidence, these three choices lead respectively to the following effective impedance formulas for medium (2):

$$Z_{\text{eff}}^{(2)} = \frac{\langle E_y^{(2)}\rangle^2}{\langle(\boldsymbol{E}^{(2)} \times \boldsymbol{H}^{(2)})\cdot \boldsymbol{e}_z\rangle}, \quad \text{(see also [3])}, \quad (3)$$

$$Z_{\text{eff}}^{(2)} = \frac{\langle(\boldsymbol{E}^{(2)} \times \boldsymbol{H}^{(2)})\cdot \boldsymbol{e}_z\rangle}{\langle H_x^{(2)}\rangle^2}, \quad \text{(see also [4])}, \quad (4)$$

$$Z_{\text{eff}}^{(2)} = \frac{\langle E_y^{(2)}\rangle}{\langle H_x^{(2)}\rangle}, \quad \text{(see also [5])}, \quad (5)$$

where the operator $\langle F\rangle$ denotes the spatial average over (over the interface of a unit cell) of a scalar field F. The computed effective impedance tends to be only weakly dependent on the choice of the projection and in this work we will use the effective impedance concept based on Eq. (3).

978-1-4673-8603-6/16/$31.00 ©2016 IEEE

III. Application to a Lossy Metamaterial

As a model of a lossy metamaterial, we consider the example of a metamaterial structure consisting of an array of layered metal-dielectric-metal pillars [6], as illustrated in Fig. 2. Figure 3 shows the computed effective index $n_{\text{eff}}^{(2)}$ and effective impedance $Z_{\text{eff}}^{(2)}$, for normal incidence by an (E_x, H_y)-polarized plane wave; the corresponding effective dielectric permittivity $\varepsilon_{x,\text{eff}}^{(2)} = n_{\text{eff}}^{(2)}/Z_{\text{eff}}^{(2)}$ and effective magnetic permeability $\mu_{y,\text{eff}} = \mu_{z,\text{eff}}^{(2)} = n_{\text{eff}}^{(2)} Z_{\text{eff}}^{(2)}$ are plotted in Fig. 4. Figure 4 indicates that the effective magnetic permeability $\mu_{y,\text{eff}}^{(2)}$ has a negative real part for frequencies $\nu \in [0.75\,\text{THz},\ 1.15\,\text{THz}]$. It follows that the vacuum-homogenized material interface can support surface modes with TE-polarization (or magnetic surface plasmon). The presence of magnetic surface plasmons implies that a metamaterial waveguide (see Fig. 5) can guide E_x-polarized waves. The field confinement near the waveguide core does not rely on total internal reflection; instead confinement is due to the existence of surface modes, so a metamaterial waveguide with a subwavelength core diameter can still confine waves. The continuous curves and dashed curves in Fig. 6 indicate respectively the dispersion curves of a planar metamaterial waveguide and its homogenized material waveguide.

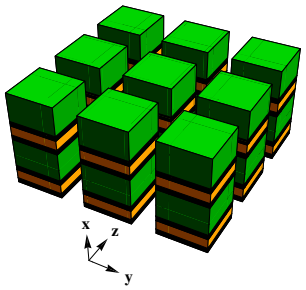

Fig. 2. Illustration of a metamaterial.

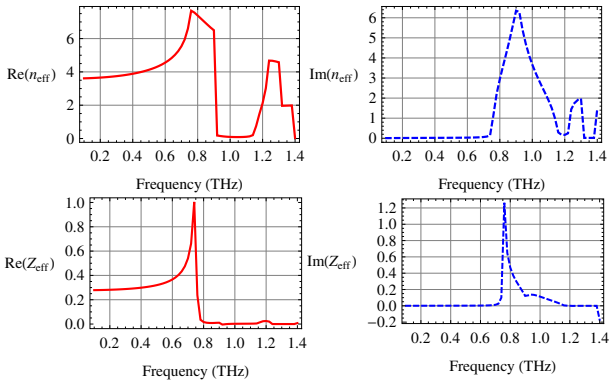

Fig. 3. The computed effective parameters $n_{\text{eff}}^{(2)}$ and $Z_{\text{eff}}^{(2)}$.

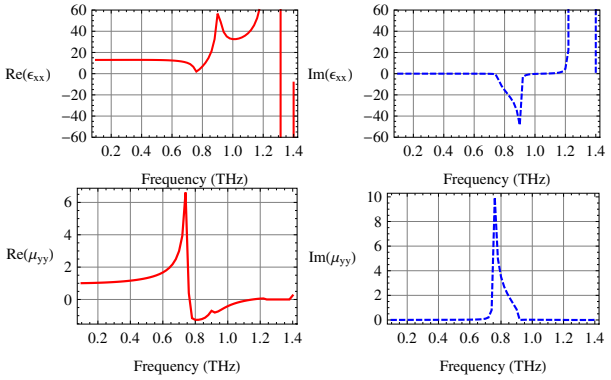

Fig. 4. The real and imaginary parts of the effective dielectric constant $\varepsilon_{x,\text{eff}}^{(2)}$ and effective magnetic permeability $\mu_{y,\text{eff}}^{(2)}$.

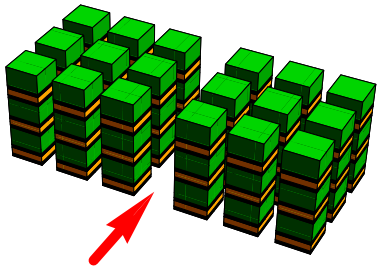

Fig. 5. Illustration of a planar waveguide with homogenized material cladding.

[1] K. B. Dossou, C. G. Poulton, and L. C. Botten, "Effective impedance modeling of metamaterial structures," *J. Opt. Soc. Am. A*, vol. 33, no. 3, pp. 361–372, 2016.

[2] K. B. Dossou, L. C. Botten, and C. G. Poulton, "Semi-analytic impedance modeling of three-dimensional photonic and metamaterial structures," *J. Opt. Soc. Am. A*, vol. 30, no. 10, pp. 2034–2047, 2013.

[3] B. Momeni, A. A. Eftekhar, and A. Adibi, "Effective impedance model for analysis of reflection at the interfaces of photonic crystals," *Opt. Lett.*, vol. 32, no. 7, pp. 778–780, 2007.

[4] B. Momeni, M. Badieirostami, and A. Adibi, "Accurate and efficient techniques for the analysis of reflection at the interfaces of three-dimensional photonic crystals," *J. Opt. Soc. Am. B*, vol. 24, no. 12, pp. 2957–2963, 2007.

[5] Z. Lu and D. W. Prather, "Calculation of effective permittivity, permeability, and surface impedance of negative-refraction photonic crystals," *Opt. Express*, vol. 15, no. 13, pp. 8340–8345, 2007.

[6] A. Ishikawa, S. Zhang, D. A. Genov, G. Bartal, and X. Zhang, "Deep subwavelength Terahertz waveguides using gap magnetic plasmon," *Phys. Rev. Lett.*, vol. 102, p. 043904, 2009.

References

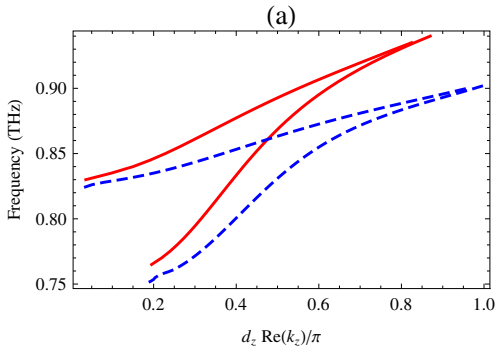

Fig. 6. The continuous and dashed curves are respectively the dispersion curves of the metamaterial waveguide and homogenized material waveguide.